processes

MDPI

Article

Numerical Simulation of Surface Gas Venthole Extraction and the Effect of Ventilation Mode in Pressure-Relief Mining

Yubo Liu, Cun Zhang * and Ziyu Song

School of Energy and Mining Engineering, China University of Mining and Technology Beijing, Beijing 100083, China; liuyubo@student.cumtb.edu.cn (Y.L.); zqt2000101037@student.cumtb.edu.cn (Z.S.)
* Correspondence: cumt-zc@cumtb.edu.cn; Tel.: +86-15810194127

Abstract: The stress-relief coal mine methane surface gas venthole is considered an effective method by which to realize coal mine methane exploitation and outburst prevention. Existing stress permeability models for caved zones, fractured zones, and bending subsidence zones were embedded into FLAC3D simulation software by using the FISH language. In cooperation with the in-situ data of a mine in a Huainan coalfield, the permeability distribution of pressure-relief surface gas drainage via different zones was simulated. The results indicated that the surface gas ventholes were effective for gas extraction from mining areas. By analyzing the distribution of permeability, three zones were identified: (1) the fully compacted zone, (2) the gradually compacted zone, and (3) the "O" type fractured zone. The seepage path of pressure-relief surface gas drainage was visualized. Most of the gas seeps into the adjacent rock mass at first and then is extracted through surface gas ventholes. Meanwhile, seepage of gas with different ventilation modes in longwall-panel, U-type, and Y-type was analyzed. Results shows that the Y-type ventilation mode is better than the U-type for gob gas control in the longwall panel. A comparison between the simulated model and the on-site recorded data is conducted, and results show that the model represents the site condition reasonably well. The simulation results provide theoretical guidance to engineering practice.

Keywords: surface gas venthole; gas seepage path; ventilation mode; pressure-relief mining

Citation: Liu, Y.; Zhang, C.; Song, Z. Numerical Simulation of Surface Gas Venthole Extraction and the Effect of Ventilation Mode in Pressure-Relief Mining. *Processes* **2022**, *10*, 750. https://doi.org/10.3390/pr10040750

Academic Editor: Adam Smoliński

Received: 13 March 2022
Accepted: 7 April 2022
Published: 13 April 2022

1. Introduction

Gas is widely present in coal fields. One of the critical issues coal mining needs to face is gas. With coal mining going deeper and larger in nowadays, gas pressure and gas content increases drastically [1,2]. A few coal mines are facing unsatisfying issues pertaining to permeability, gas pressure, and gas saturation, and these problems become barriers to gas extraction [3,4]. Surface gas venthole (SGV) is a successful technology applied to pressure-relief coal mine methane (CMM) and outburst prevention [5–7]. SGV aims at collecting methane in the gob and protected coal seams prior to the methane getting into the work environment by drilling into the gob where protective coal-seam mining is conducted, as shown in Figure 1. Good methane control will benefit underground safety and use methane as a clean fuel. Many attempts, such as theoretical analysis, field trials, and numerical and laboratory simulations, have been conducted to evaluate SGV performance, and the parameters could affect SGV [8–13].

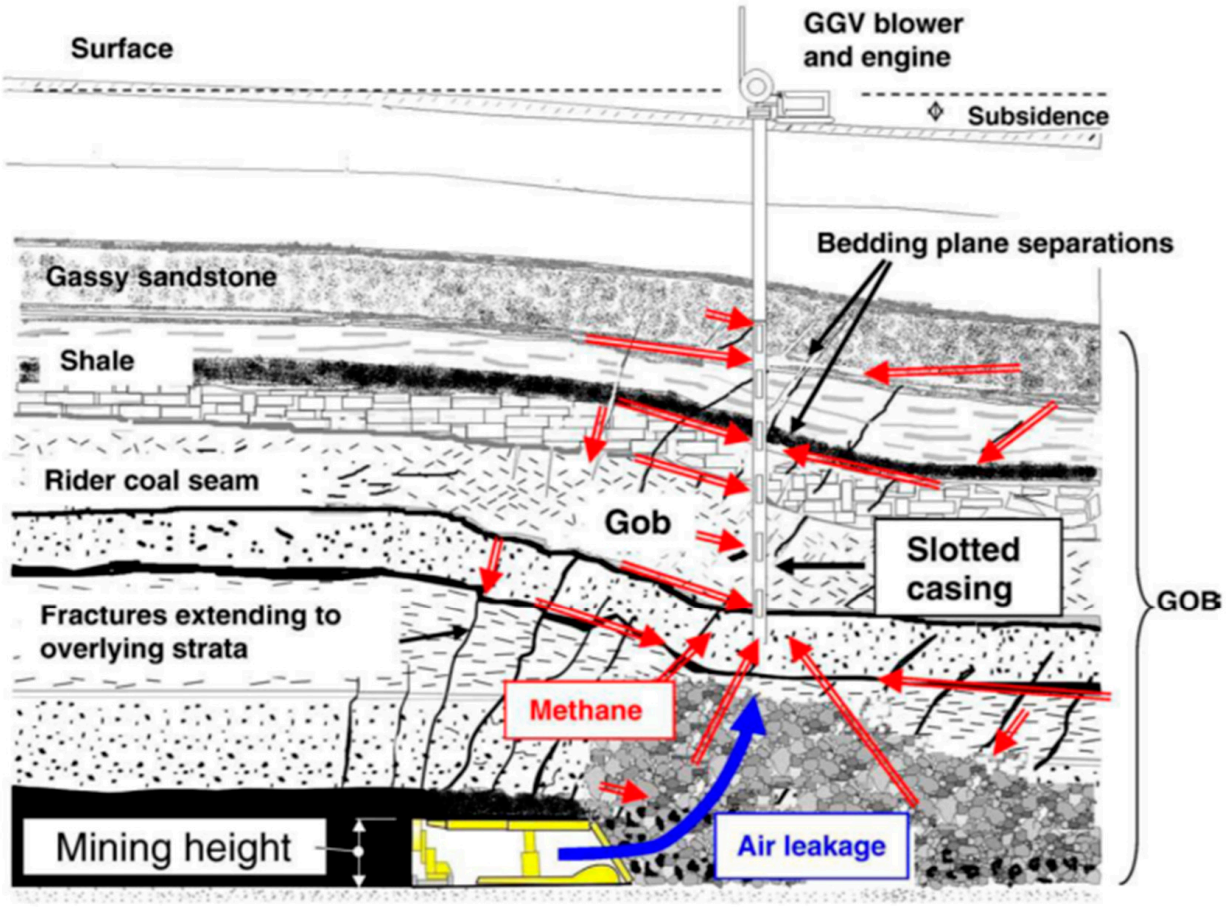

Figure 1. Schematic diagram of surface GGV [14].

The key consideration of methane control in coal mines is permeability and its anisotropy characteristics [15–17]. The anisotropy of permeability is dominated by in-situ structural conditions and corresponding stress distribution [12,18]. Upon exploiting activities, there is a clear zoning phenomenon of permeability [19]. The arrangement of SGVs is closely related to the permeability distribution. Currently, field measurement can hardly be an ideal means by which to evaluate the performance of SGV because of its high cost. Simulated experimentation is mainly focused on analyzing fracture evolution and displacement of protective seams' roof and floor, as well as stress changes of protected seams and permeability changes of protective seams. It is hard to undertake fluid–solid coupling mechanics analysis because the cost is even higher. Therefore, numerical simulation is often applied to studies given the cheap financial cost and good performance. Moreover, numerical simulation provides a means by which to quantitatively analyze individual factors among all the parameters. By properly selecting input parameters, numerical simulation can generate very trustworthy results when compared with field measurement. Thus, it has been utilized by many scholars as a main tool with which to conduct research with respect to mining and factor analysis. Many current evaluations use indirect parameters such as stress relief, fracture evolution, and failure zones. Although these parameters provide insight into the performance of methane extraction, they can hardly address the evolution of permeability; thus difficulties arise when attempts are made to calculate seepage in mining activities [20–23]. In terms of gas flow and drainage simulation, the evolution of permeability and gas seepage during pressure relief mining is difficult to obtain by using theoretical predictions [10,24–27]. In addition, the ventilation mode of a longwall face has a great impact on the air leakage in goaf [28], and it has a great impact on the gas

concentration of SGV extraction; however those issues have not drawn much attention in research.

In general, the performance of SGVs depends on the permeability of applied strata. As for the evaluation of permeability, numerical modelling has significant advantages over many other approaches. It is possible to study the performance of SGVs by properly addressing a numerical model [29]. Based on the study by [30,31], An algorithm to study the reservoir model by using the FISH language was carried out by [32,33], through which the permeability at different zones in the mining process can be calculated. In this paper, existing stress permeability models for caved zones, fractured zones, and bending subsidence zones were embedded into FLAC3D simulation software by using the FISH language. In cooperation with the in-situ data of a mine in the Huainan coalfield, the permeability distribution of pressure relief surface gas drainage via different zones was simulated, and the extraction process of SGV may also further controlled. Based on this, the influence factors of the ventilation mode in the longwall face were also studied in this paper. Finally, a comparison between the simulated model and on-site recorded data is conducted.

2. Rock Permeability and Its Calculation

As shown in Figure 2, pressure-relief mining can initiate the surrounding rock to be damaged. The damage content is related to the distance between the rock and a longwall panel. A closer distance will generate bigger damage. Rock and coal permeability changes in the model can be calculated by using the model proposed by [32,33]. According to the exponential relationship between rock mass permeability and stress (Equation (1)), the relationship between the rock mass permeability and stress of the intact, fractured, and broken rock can be calculated by laboratory testing, as shown in Table 1. Thus we get

$$k_1 = k_0 e^{-3\frac{c_{f0}}{\alpha_f}(1-e^{-\alpha_f \sigma_e})} \quad (1)$$

where k_1 stands for the permeability with effective stress equal to σ_e and k_0 is the original permeability, c_f is the fracture compressibility, α_f stands for the changing rate of fracture compressibility, and c_{f0} stands for the initial fracture compressibility.

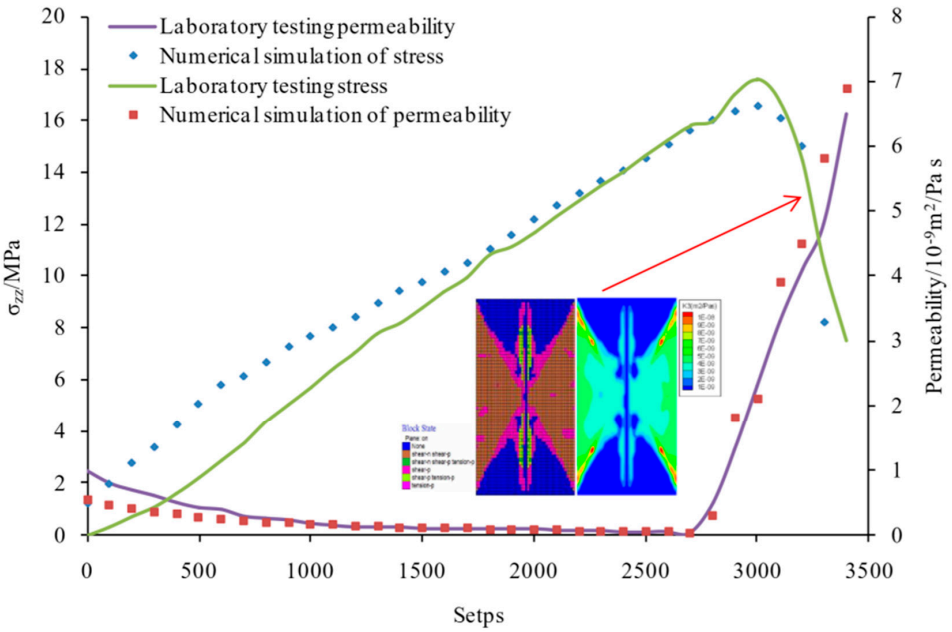

Figure 2. Modelling results of uniaxial compression and permeability-stress change curve [34].

Table 1. Laboratory test results of different permeability models.

Sample Type	Parameters			Models	R^2
	k_{f0} (md)	c_{f0} (MPa^{-1})	α_f (MPa^{-1})		
Raw sample	5.1733	0.3450	0.1247	$k_1 = 5.17e^{-8.30(1-e^{-0.14\sigma_1})}$	0.9963
Fracture sample	116.0769	0.1925	0.0386	$k_1 = 116.08^{-14.96(1-e^{-0.04\sigma_1})}$	0.9915
Broken rock sample	336.0769	0.0740	0.2996	$k_1 = 336.08e^{-0.82(1-e^{-0.27\sigma_1})}$	0.9934

3. Introduction to the Studied Longwall Face

The studied object in this paper is the longwall face 1242(1), and it is conducted at the Huainan coalfield. The longwall face 1242(1) belongs to the 11-2 coal seam (protective coal seam). The depth of the 11-2 coal seam is 930 m and the thickness is on average 1.2 m. The nearest above coal seam is the 13-1 coal seam (protected coal seam) and its vertical distance is on average 66 m. According to site investigation, the gas content of the 11-2 coal seam is 4.73 m^3/t, and the pressure can reach 0.5 MPa top. The 13-1 coal seam faces more intense gas conditions with a maximum gas pressure of 3.7 MPa, and gas content of 8.08 m^3/t. Seven SGVs were arranged to study the longwall face 1242(1). The total length of SGVs is 1315 m and the dip length is 220 m. The arrangement of SGVs is shown in Figure 3.

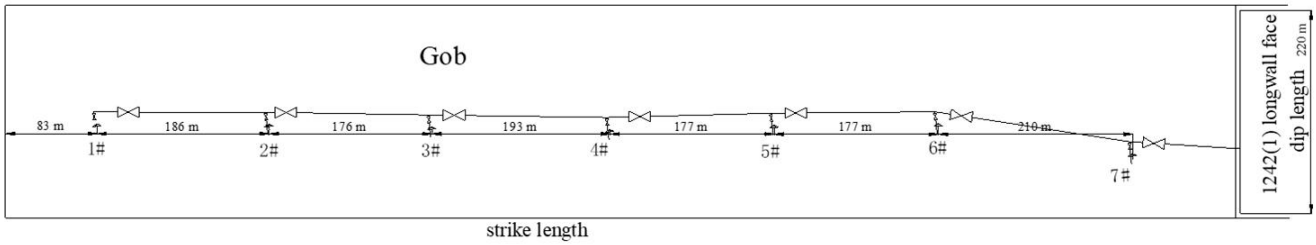

Figure 3. SGV stations in LW1242(1) panel in the Huainan coalfield [34].

4. Numerical Modelling of SGV Extraction

4.1. Basic Assumption of Modelling

The length in X, Y, and Z direction was defined to be 300 m, 400 m, and 500 m, respectively, as per the size of face1242(1). The dip length of 1242(1) was 220 m. As per the site engineering design, the height of the drifts was defined to be 2.5 m and the width was 5 m. The failure criteria used in the numerical modelling for the gob was an elastic model. The modified bulk modulus of the gob is as according to Equation (2). Two SGVs were arranged in the model according to the actual situation on site, as shown in Figure 4. Thus we get

$$K = \frac{4G}{3} = \frac{\sigma_v}{2\varepsilon} = \frac{E_0}{2\,(1-\varepsilon/\varepsilon_m)} \quad (2)$$

where K represents bulk modulus, G is shear modulus, σ_v refers to vertical stress, E_0 is elasticity modulus, ε stands for vertical strain, and ε_m refers to maximum vertical strain.

4.2. Surrounding Rock Permeability Distribution

Simulation panel every 5 m for a mining step, mechanical calculation and continuous upgrading of surrounding rock permeability is conducted in every step. After permeability calculation, the extraction process of SGV was simulated. The panel in the model had been advancing 300 m. After the mining, the simulation results were imported to TECPLOT for post-processing.

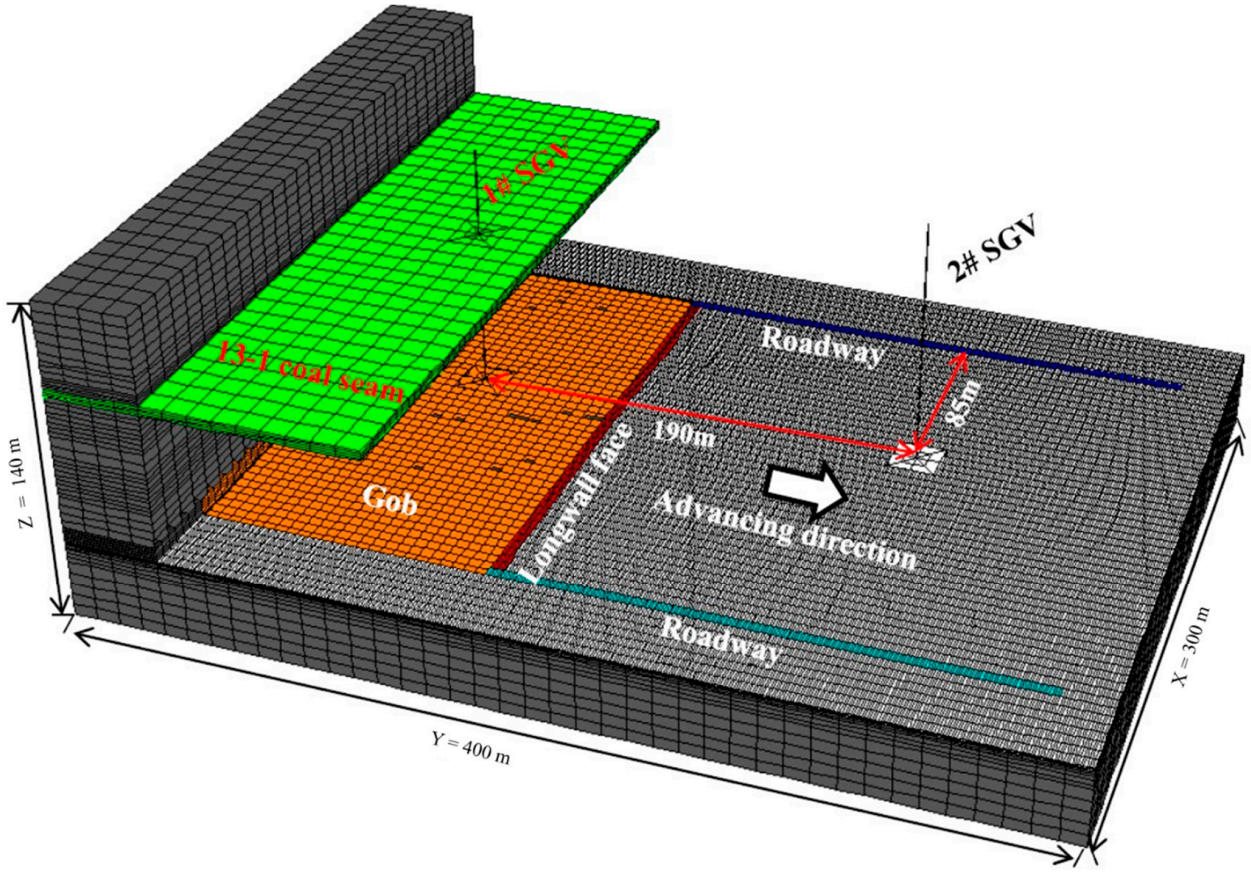

Figure 4. Numerical model of longwall face 1242(1) [34].

The strata above the mining seam can be categorized into four zones vertically: (1) the surface zone, (2) the constrained zone, (3) the fractured zone, and (4) the caved zone from top to the bottom, and the permeability differs from zone to zone, as shown in Figure 5. Figure 6 shows the contour plotting of permeability distribution on the longitudinal cut plane of the model corresponding to Figure 5. It can be seen from Figure 6 that the permeability of the caved zone in the goaf is the largest, and the permeability of the fractured zone at the left and right ends in the fractured zone is the second largest. The permeability in the compacted area in the middle of the fractured zone is less than that in the uncompacted area at both ends, but it is still in the same order of magnitude. The permeability of the surrounding rock is generally increased in combination with the "funnel" structure, which shows that the permeability of the whole protected coal seam can be greatly increased. Figure 7 shows the contour plotting of permeability distribution on the cross-cut plane of the protected coal seam. The permeability of the protected coal seam is generally O-shaped from inside to outside, and there is an obvious zoning phenomenon. From inside to outside, there is a fully compacted zone, an incompletely compacted zone, and an O-shaped fracture zone, and the permeability increases gradually. Compared with the original permeability of the protected coal seam, the permeability after pressure relief increases by more than 1000 times. The simulation results of permeability distribution indicates an obvious effect in protective seam mining: permeability enhancement and pressure-relief effect.

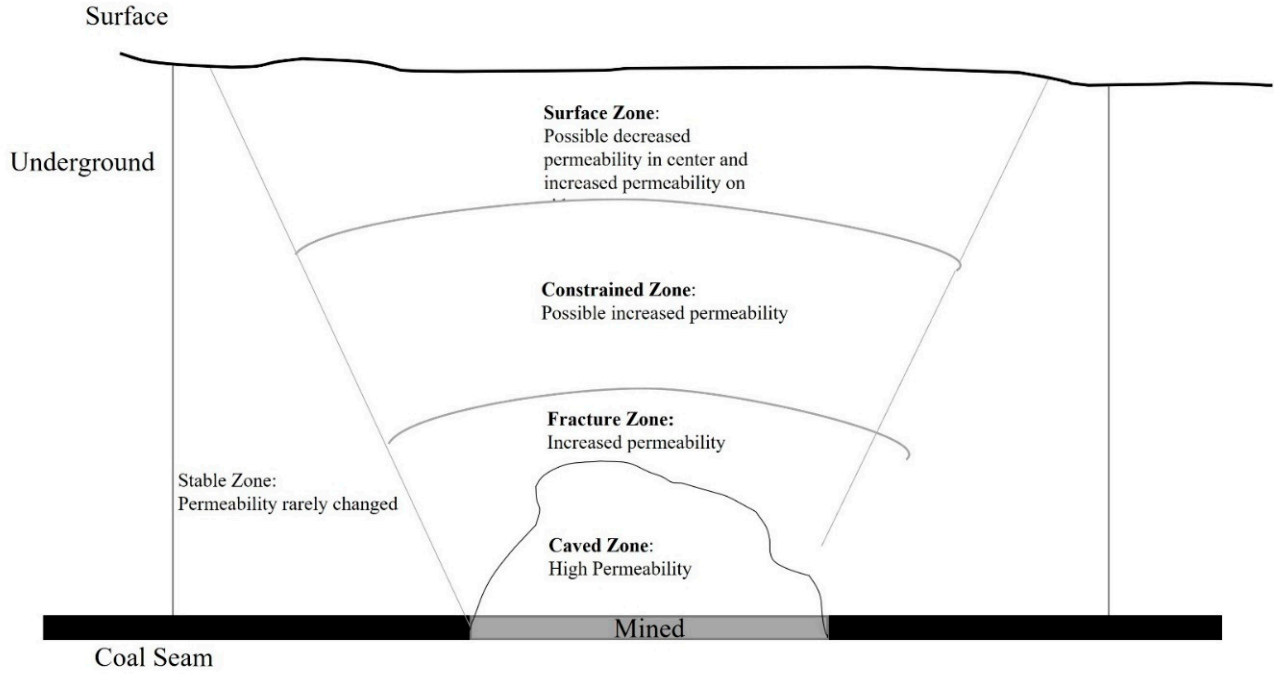

Figure 5. Schematic diagram of hydrogeological model for mined coal seam area, after [35].

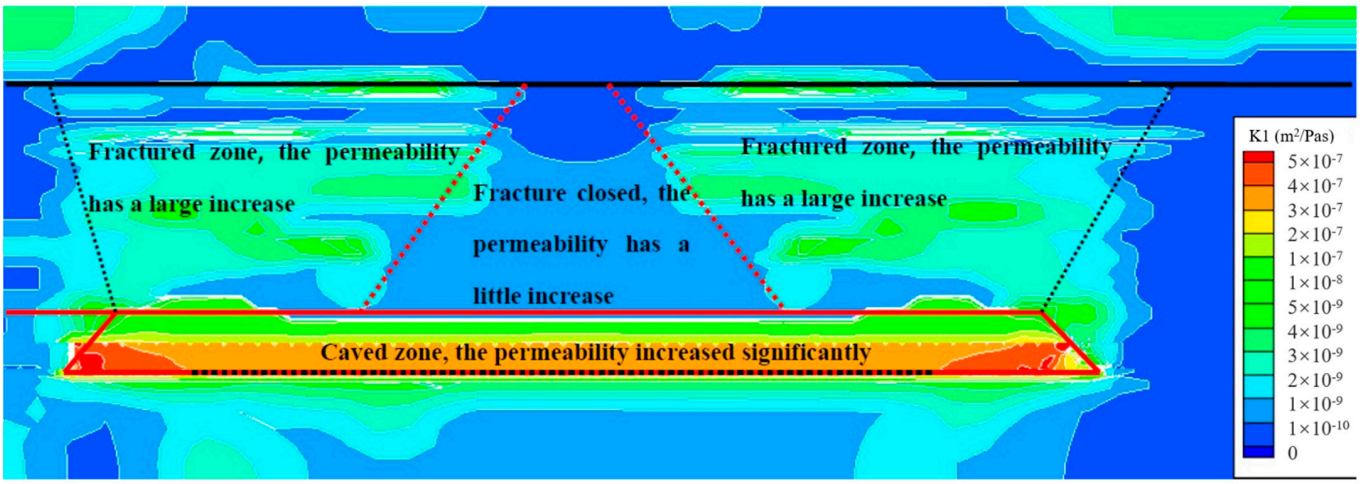

Figure 6. The contour plotting of permeability distribution on longitudinal cut plane of model.

4.3. The Performance of SGV Extraction

In terms of evaluating the performance of SGV extraction, the flow simulation with and without SGV in the same time steps were implemented in this paper. The simulation results were shown in Figure 8. The pressure-relief gas from the protected coal seam inrushed into the adjacent rock strata in protective coal seam mining due to the enhancement of permeability. The gas pressure decreased because the protected coal seam with SGV extraction was larger than without SGV extraction, especially in the middle of the compaction zone (Figure 8). The gas pressure will decrease from 3.5 MPa to about 1.5 MPa. Due to the SGV extraction, gas pressure decreases obviously around SGV. It is able to extract the pressure-relief gas from the fractured zone to accelerate the gas pressure decreasing of the protected coal seam. In general, SGV is a successful approach to maintain the safety of mining for protective seams and realize the coal and gas simultaneous extraction.

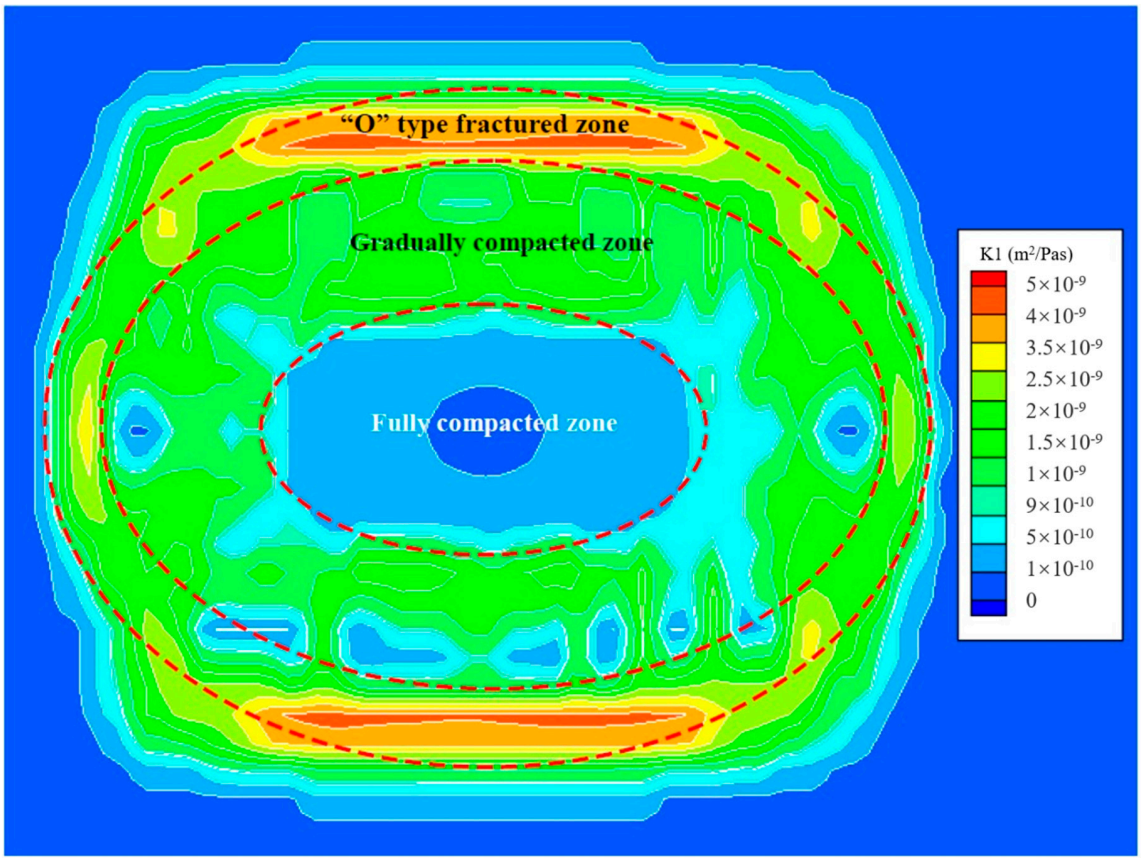

Figure 7. The contour plotting of permeability distribution in protected coal seam.

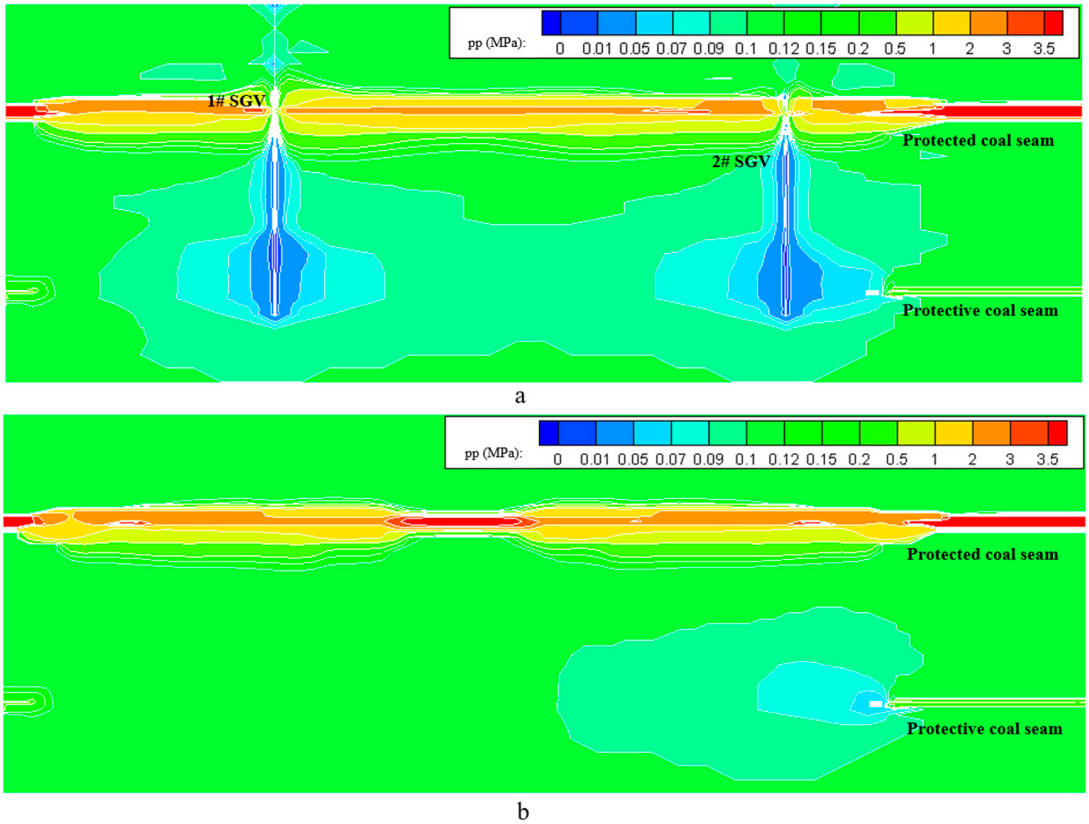

Figure 8. Gas pressure distribution, (**a**,**b**) is with and without SGV respectively.

4.4. The Seepage Path of Pressure Relief Surface Gas in SGV Extraction

The gas seepage path in the gob and around the SGV during gas extraction was shown in Figure 9. The extraction area of the 1# SGV and 2# SGV in the gob was overlapping (Figure 9a). The extraction drill hole close to the panel, 2# SGV, had the larger extraction area because of the high permeability around the 2# SGV. However, though the extraction rates of the 2# SGV were larger than 1# SGV, the methane concentration was relatively low due to the large quantity of air extracted (Figure 9a). As shown in Figure 9b, the gas extraction mainly came from the fractured zone between protective and protected coal seams. The main assumptions as follows. (1) The extraction area and average permeability of the fractured zone between the protective and protected coal seams was larger than the protected coal seam. (2) The gas content around SGV reduced gradually due to the gas extraction and pressure-relief gas emission. The gas pressure of the fractured zone decreased slowly because of the replenishment of the protected coal seam. In order to verify the above assumptions, the monitoring points including 1# (caved zone), 2# (fractured zone close to the caved zone), 3# (fractured zone close to the protected coal seam) and 4# (protected coal seam) were arranged in the model during the gas extraction simulation. The monitored results were illustrated in Figure 10.

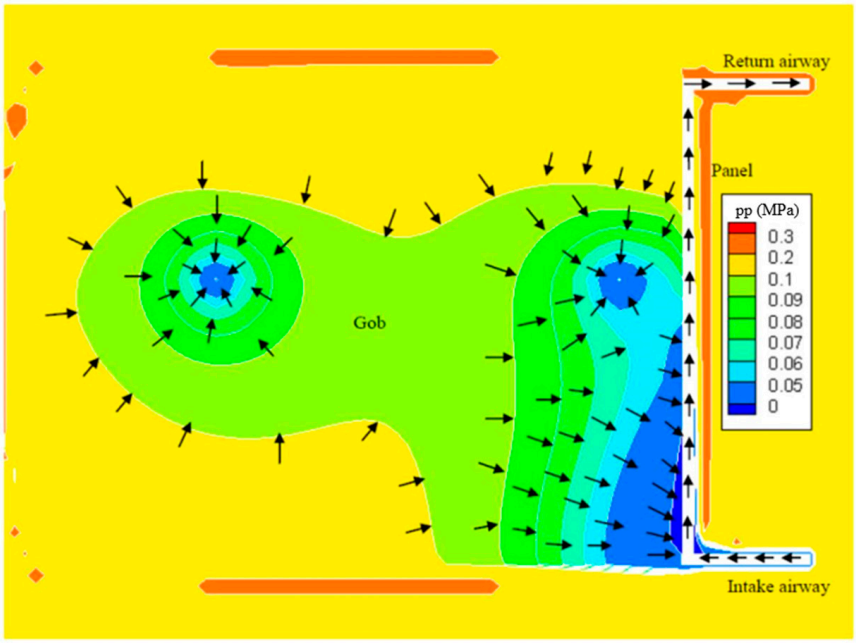

a

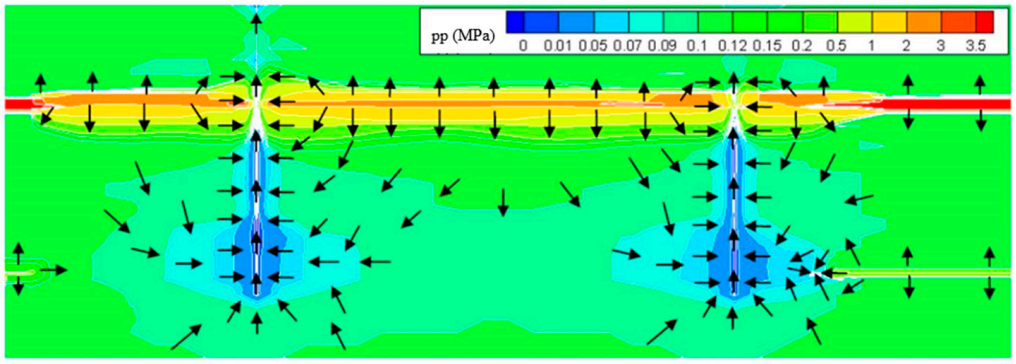

b

Figure 9. Gas seepage path in the process of extraction. (**a**) Gob section. (**b**) SGV section.

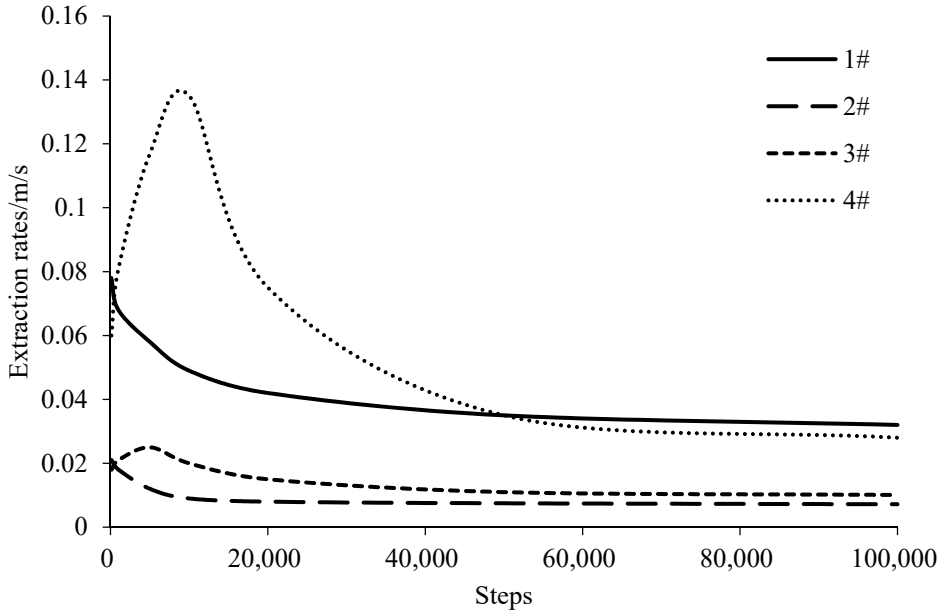

Figure 10. Gas flow rates variation curve of the monitoring points.

At the beginning of extraction work, the extraction rates of 1# monitoring points were the largest and decreased quickly due to the gob compaction. Monitoring points of 2 # had the same changing trend with the 1#, but the extraction rates decreased slowly because of the replenishment of the protected coal seam. The changing trend of extraction rates to 3# and 4# were the same, increasing at the beginning of the extraction and then decreasing. The increasing of the extraction rates caused by the protective panel advancing and the more pressure-relief gas gushed into the fractured zone [31]. Corresponding to the above assumptions, the extraction rates of 2# decreased slower than 1# and the extraction rates of 3# increased at the beginning. The slow decrease of pressure relief gas was because of the protected coal seam replenishment. Although the extraction rates of 4# were larger than 2# and 3# during the SGV extraction, the extraction area of the fractured zone between protective and protected coal seam was larger than the protected coal seam. Thus, the total volume of extraction from the fractured zone is larger than protected coal seam.

In general, except for extracting from the protected coal seam, most of the gas first seeps to the adjacent rock mass and then is extracted by SGV. These simulation results are basically consistent with the theoretical analysis, physical simulation, field test, and laboratory test results described in this paper and other papers [36–39].

4.5. The Effect of Ventilation Mode

There are two ventilation modes used in the Huainan coalfield: U-type and Y-type. The main influence of ventilation modes on the SGV extraction is the performance of the caved zone extraction. The parameters in these two modellings were unchanged, but the ventilation mode and the results were shown in Figure 11. It is important to note that the gob was enclosed by the gob-side entry retaining, around which the permeability was very low. Onsite engineering production requires the extraction pipes to be buried into the gob to extract the gas during mining. In order to reflect the buried pipe extraction, the gob-side entry retaining was assigned a negative pressure to extract the gas. Because of the two-intake airway of the Y-type ventilation mode, the gas in the upper corner of the panel is relatively lower than U-type (Figure 11). Moreover, the gas extraction in the gob-side entry retaining can: (1) make the gas pressure largely decrease in the gob, which is closed to the retained drifts; and (2) increase the extraction radius of the SGV. The above results indicated that the Y-type ventilation mode is better than U-type for gob gas control in the longwall panel. The utilized model showed good potential for the application to site productions regarding the evaluation of ventilation and the choice of ventilation mode.

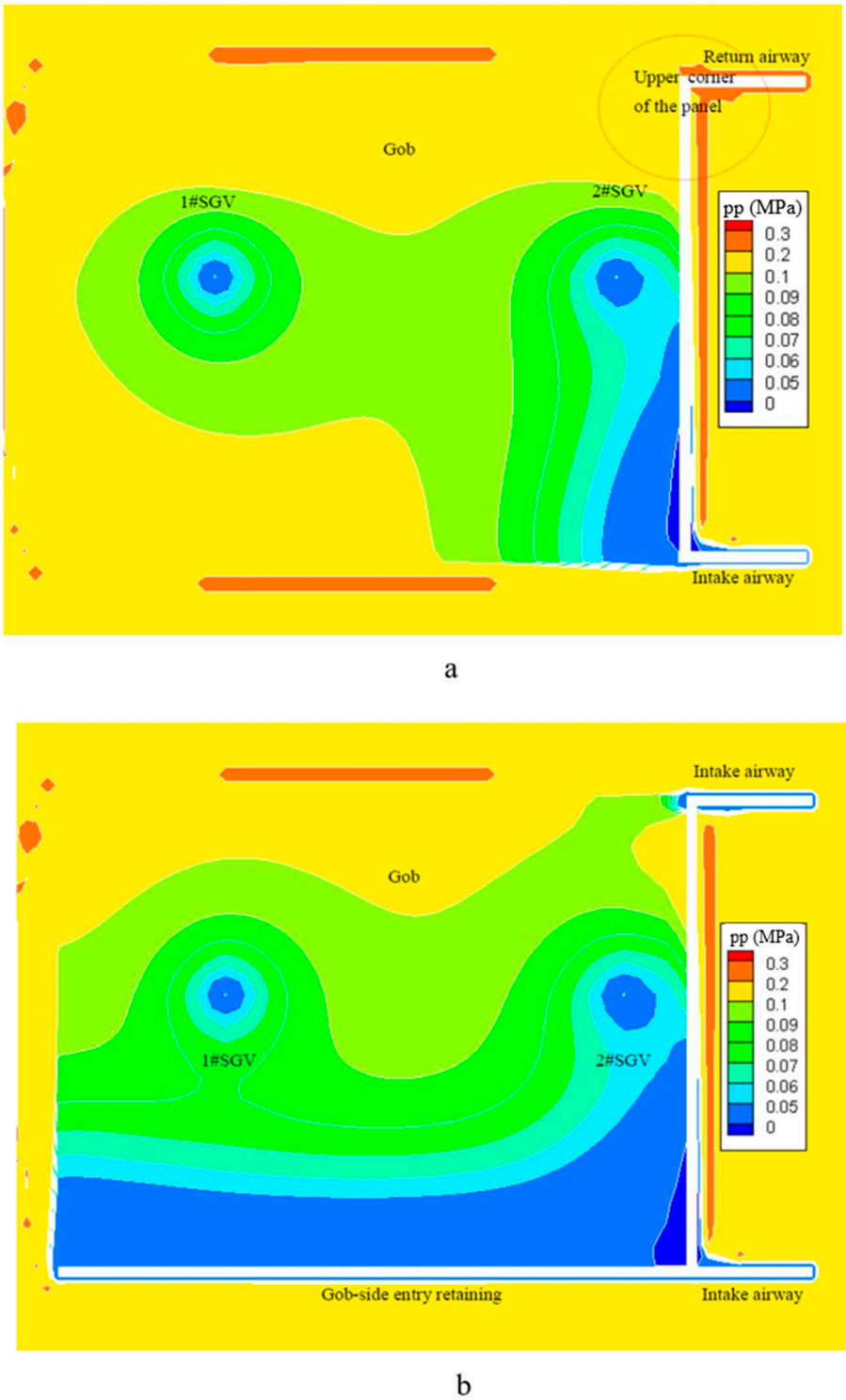

Figure 11. The gas pressure distribution in the gob with different ventilation mode. (**a**) U-type. (**b**) Y-type.

5. Site Validation

The production data of the 1# and 2# SGV were recorded in the whole mining process, and the gas extraction rates and the methane concentration were shown in Figure 12. Three stages were witnessed in Figure 12 in terms of the evolution of methane flow rate: (1) sharp climbing, (2) gradual declining, and (3) relative stability. Those stages were similar to the 3# and 4# monitoring points in Figure 10. Due to the low methane concentration of the gob gas extraction, the results in Figure 12 are similar to Figure 10 and were very powerful

proof of the reliability of the simulation. Besides, the methane concentration is relatively small at the beginning of the SGV extraction corresponding to the analysis of Figure 9. The methane concentration was relatively low due to the large quantity of air extracted (Figure 9a). In summary, the numerical model can be regarded as representative of the actual mining conditions of protective seams.

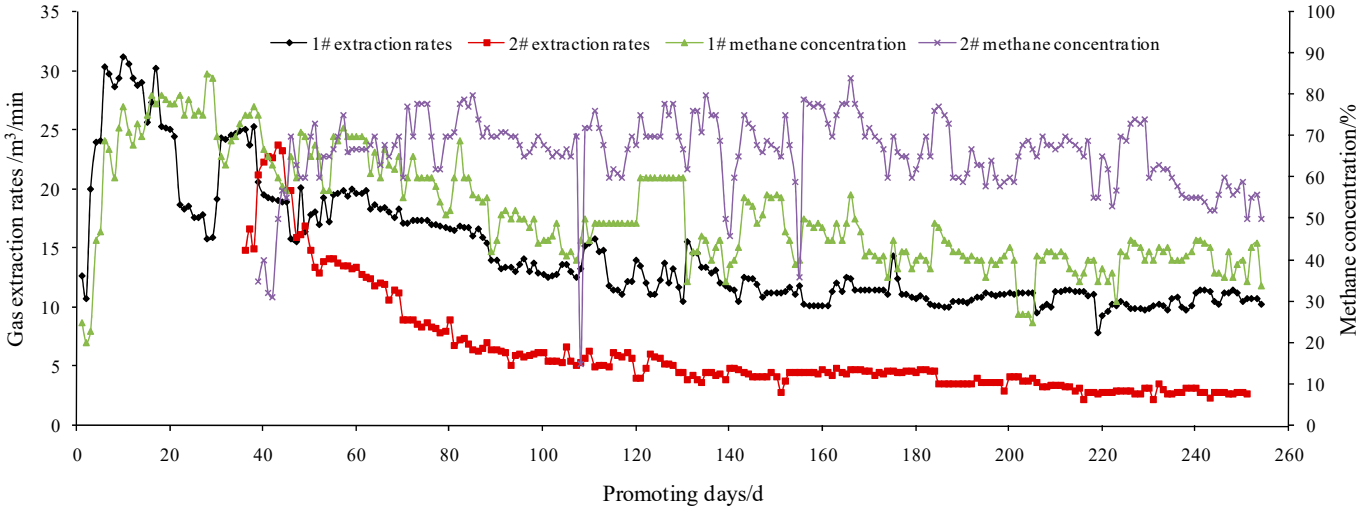

Figure 12. Gas extraction data of surface gas venthole.

6. Discussions and Conclusions

In this paper, existing stress permeability models for caved zones, fractured zones, and bending subsidence zones were embedded into FLAC3D simulation software by using the FISH language. The permeability distribution of pressure relief surface gas drainage via different zones was simulated, and the extraction process of SGV was further controlled. Based on this, the influence factors of the ventilation mode in the longwall face were also studied in this paper. Thus, this study enhances the understanding of permeability distribution after extraction and provides suggestions on the arrangement of SGVs. The compared results between the U-type and Y-type ventilation mode will provide useful suggestions on the choice of ventilation mode. However, in our work, the permeability models and the associated parameters are obtained from various experiments with specific rock mass; therefore, each model should have its accommodation. It is debatable whether these models should be utilized without calibrations, which may reduce the reliability of the simulation. Moreover, pressure relief mining produces loading and unloading processes in the protected coal seam, and we also find the permeability heavily depends on the loading or unloading process, i.e., permeability is stress path dependence [40,41]. Thus, in our future work, the effect of loading and unloading path on permeability will be studied. Moreover, more ventilation models will be studied subsequently. The main conclusions of this paper are as follows:

Incorporated with the in-situ conditions from a mine of the Huainan coalfield, the permeability distribution in the process of pressure relief surface gas drainage was simulated by using numerical simulation. The results indicated that the permeability of the caved zone was the largest and increased from the inside to the outside of the caved zone. There was an obvious zoning phenomenon of the permeability distribution in the fractured zone. They can be divided as (1) the fully compacted zone, (2) the gradually compacted zone, and (3) the "O" type fractured zone. The categorized zones were generally in line with the concept proposed by [32]. The simulated model showed great potential to represent the permeability distribution.

The flow simulation with and without SGV in the same time steps witnessed the well performance of SGV in terms of preventing gas outburst hazard. Moreover, seepage path of

pressure relief surface gas drainage was obtained. Most of the gas seepage to the adjacent rock mass occurred first and was then finally extracted by surface gas venthole.

By contrast, the simulation results show that the Y-type ventilation mode is better than U-type for gob gas control in the longwall panel. The U-type ventilation mode not only made the gas pressure largely decrease in the gob which closed to the retained drifts but also increased the extraction radius of the SGV.

Author Contributions: Conceptualization, Y.L. and C.Z.; methodology, C.Z.; software, Z.S.; validation, Y.L.; formal analysis, Y.L.; investigation, Y.L. and Z.S.; resources, C.Z.; data curation, Z.S.; writing—original draft preparation, Y.L.; writing—review and editing, C.Z.; visualization, Z.S.; supervision, C.Z.; project administration, C.Z.; funding acquisition, C.Z. All authors have read and agreed to the published version of the manuscript.

Funding: Financial support for this work was provided by the National Natural Science Foundation of China (U1910206, 51904011, 52104155), the Natural Science Foundation of Beijing (8212032), and the Open Fund of State Key Laboratory of Mining-induced Response and Disaster Prevention and Control in Deep Coal Mines (SKLMRDPC19KF08).

Data Availability Statement: The data presented in this study are available on request from the corresponding author.

Conflicts of Interest: The authors declare no conflict of interest.

References

1. Wang, H.; Cheng, Y.; Yuan, L. Gas outburst disasters and the mining technology of key protective seam in coal seam group in the Huainan coalfield. *Nat. Hazards* **2013**, *67*, 763–782. [CrossRef]
2. Guo, B.; Li, Y.; Jiao, F.; Luo, T.; Ma, Q. Experimental study on coal and gas outburst and the variation characteristics of gas pressure. *Géoméch. Geophys. Geo-Energy Geo-Resour.* **2018**, *4*, 355–368. [CrossRef]
3. Jiang, J.Y.; Cheng, Y.P.; Wang, L.; Li, W.; Wang, L. Petrographic and geochemical effects of sill intrusions on coal and their implications for gas outbursts in the Wolonghu Mine, Huaibei Coalfield, China. *Int. J. Coal Geol.* **2011**, *88*, 55–66. [CrossRef]
4. Zhang, C.; Zhang, L.; Tu, S.; Hao, D.; Teng, T. Experimental and Numerical Study of the Influence of Gas Pressure on Gas Permeability in Pressure Relief Gas Drainage. *Transp. Porous Media* **2018**, *124*, 995–1015. [CrossRef]
5. Karacan, C.Ö.; Ruiz, F.A.; Cotè, M.; Phipps, S. Coal mine methane: A review of capture and utilization practices with benefits to mining safety and to greenhouse gas reduction. *Int. J. Coal Geol.* **2011**, *86*, 121–156. [CrossRef]
6. Sang, S.; Xu, H.; Fang, L.; Li, G.; Huang, H. Stress relief coalbed methane drainage by surface vertical wells in China. *Int. J. Coal Geol.* **2010**, *82*, 196–203. [CrossRef]
7. Chang, X.; Tian, H. Technical scheme and application of pressure-relief gas extraction in multi-coal seam mining region. *Int. J. Min. Sci. Technol.* **2018**, *28*, 483–489.
8. Karacan, C.Ö.; Luxbacher, K. Stochastic modeling of gob gas venthole production performances in active and completed longwall panels of coal mines. *Int. J. Coal Geol.* **2010**, *84*, 125–140. [CrossRef]
9. Schatzel, S.J.; Karacan, C.Ö.; Dougherty, H.; Goodman, G.V. An analysis of reservoir conditions and responses in longwall panel overburden during mining and its effect on gob gas well performance. *Eng. Geol.* **2012**, *127*, 65–74. [CrossRef]
10. Liu, Y.; Shao, S.; Wang, X.; Chang, L.; Cui, G.; Zhou, F. Gas flow analysis for the impact of gob gas ventholes on coalbed methane drainage from a longwall gob. *J. Nat. Gas Sci. Eng.* **2016**, *36*, 1312–1325. [CrossRef]
11. Ren, D.; Zhou, D.; Liu, D.; Dong, F.; Ma, S.; Huang, H. Formation mechanism of the Upper Triassic Yanchang Formation tight sandstone reservoir in Ordos Basin—Take Chang 6 reservoir in Jiyuan oil field as an example. *J. Pet. Sci. Eng.* **2019**, *178*, 497–505. [CrossRef]
12. Liu, Q.; Chu, P.; Zhu, J.; Cheng, Y.; Wang, D.; Lu, Y.; Liu, Y.; Xia, L.; Wang, L. Numerical assessment of the critical factors in determining coal seam permeability based on the field data. *J. Nat. Gas Sci. Eng.* **2020**, *74*, 103098. [CrossRef]
13. Zuber, M.D. Production characteristics and reservoir analysis of coalbed methane reservoirs. *Int. J. Coal Geol.* **1998**, *38*, 27–45. [CrossRef]
14. Karacan, C.Ö. Reconciling longwall gob gas reservoirs and venthole production performances using multiple rate drawdown well test analysis. *Int. J. Coal Geol.* **2009**, *80*, 181–195. [CrossRef]
15. Schwartz, B.; Huffman, K.; Thornton, D.; Elsworth, D. A strain based approach to calculate disparities in pore structure between shale basins during permeability evolution. *J. Nat. Gas Sci. Eng.* **2019**, *68*, 102893. [CrossRef]
16. Guo, D.; Lv, P.; Zhao, J.; Zhang, C. Research progress on permeability improvement mechanisms and technologies of coalbed deep-hole cumulative blasting. *Int. J. Coal Sci. Technol.* **2020**, *7*, 329–336. [CrossRef]
17. Liu, T.; Lin, B.; Fu, X.; Liu, A. Mechanical criterion for coal and gas outburst: A perspective from multiphysics coupling. *Int. J. Coal Sci. Technol.* **2021**, *8*, 1423–1435. [CrossRef]

18. Lou, Z.; Wang, K.; Zang, J.; Zhao, W.; Qin, B.; Kan, T. Effects of permeability anisotropy on coal mine methane drainage performance. *J. Nat. Gas Sci. Eng.* **2021**, *86*, 103733. [CrossRef]
19. Hu, S.; Zhou, F.; Liu, Y.; Xia, T. Effective Stress and Permeability Redistributions Induced by Successive Roadway and Borehole Excavations. *Rock Mech. Rock Eng.* **2015**, *48*, 319–332. [CrossRef]
20. Bai, Q.; Tu, S.; Wang, C. Numerical simulation on top-coal arching mechanism. *J. Min. Saf. Eng.* **2014**, *31*, 208–214, (In Chinese with English Abstract).
21. Rabe, C.; Perdomo, P.R.R.; Roux, P.-F.; Silva, C.G.; Gamboa, L.A.P. Coupled fluid flow and geomechanics: A case study in Faja del Orinoco. *Géoméch. Geophys. Geo-Energy Geo-Resour.* **2020**, *6*, 1–23. [CrossRef]
22. Sun, Q.; Mu, Y.; Yang, X. Study on "two-zone" height of overlying of fully-mechanized technology with high mining thickness at Hongliu Coal Mine. *J. China Coal Soc.* **2013**, *38*, 283–286.
23. Zhang, J.; Wang, J. Similar simulation and practical research on the mining overburden roof strata "three-zones" height. *J. Min. Saf. Eng.* **2014**, *31*, 249–254.
24. Fan, C.; Elsworth, D.; Li, S.; Chen, Z.; Luo, M.; Song, Y.; Zhang, H. Modelling and optimization of enhanced coalbed methane recovery using CO_2/N_2 mixtures. *Fuel* **2019**, *253*, 1114–1129. [CrossRef]
25. Qin, J.; Yuan, L.; Guo, H.; Qu, Q. Investigation of longwall goaf gas flows and borehole drainage performance by CFD simulation. *Int. J. Coal Geol.* **2015**, *150*, 51–63. [CrossRef]
26. Ren, T.; Edwards, J. Goaf gas modeling techniques to maximize methane capture from surface gob wells. In *Mine Ventilation*; CRC Press Taylor & Francis Group: Boca Raton, FL, USA, 2002; pp. 279–286.
27. Tang, M.; Jiang, B.; Zhang, R.; Yin, Z.; Dai, G. Numerical analysis on the influence of gas extraction on air leakage in the gob. *J. Nat. Gas Sci. Eng.* **2016**, *33*, 278–286. [CrossRef]
28. Zhang, C.; Tu, S.; Zhao, Y. Compaction characteristics of the caving zone in a longwall goaf: A review. *Environ. Earth Sci.* **2019**, *78*, 27. [CrossRef]
29. Zhang, C.; Tu, S.; Yuan, Y.; Bai, Q. Numerical simulation of surface gas venthole extraction in pressure relief mining. *J. China Coal Soc.* **2015**, *40*, 392–400.
30. Esterhuizen, G.S.; Karacan, C.Ö. Development of numerical models to investigate permeability changes and gas emission around longwall mining panels. In Proceedings of the 40th U.S. Symposium on Rock Mechanics, Anchorage, AK, USA, 25–29 June 2005; pp. 25–26.
31. Whittlesa, D.N.; Lowndesa, I.S.; Kingmana, S.W.; Yates, C.; Jobling, S. Influence of geotechnical factors on gas flow experienced in a UK longwall coal mine panel. *Int. J. Rock Mech. Min. Sci.* **2006**, *43*, 369–387. [CrossRef]
32. Zhang, C.; Tu, S.H.; Zhang, L.; Wang, F.T.; Bai, Q.S. The numerical simulation of permeability rules inprotective seam mining. *Int. J. Oil Gas Coal Technol.* **2016**, *13*, 243–259. [CrossRef]
33. Zhang, C.; Bai, Q.; Chen, Y. Using stress path-dependent permeability law to evaluate permeability enhancement and coalbed methane flow in protected coal seam: A case study. *Géoméch. Geophys. Geo-Energy Geo-Resour.* **2020**, *6*, 1–25. [CrossRef]
34. Zhang, C.; Tu, S.H.; Zhang, L.; Bai, Q.S.; Yuan, Y.; Wang, F.T. A methodology for determining the evolution law of gob permeability and its distributions in longwall coal mines. *J. Geophys. Eng.* **2016**, *13*, 181–193. [CrossRef]
35. Forster, I.; Enever, J. *Hydrogeological Response of Overburden Strata to Underground Mining*; Report 1; Office of Energy: Sydney, Australia, 1992; 104p.
36. Chen, J.G.; Xu, P.; Lai, Y.X.; Du, Y.H. Research on dynamic variation effect of coal reservoirs permeability. *Rock Soil Mech.* **2011**, *32*, 2512–2516.
37. Coletta, M.; Sicco, M. Permeability increase in Bowen Basin coal as a result of matrix shrinkage during primary depletion. *Int. J. Coal Geol.* **2012**, *96–97*, 109–119.
38. Clarkson, C.; Salmachi, A. Rate-transient analysis of an undersaturated CBM reservoir in Australia: Accounting for effective permeability changes above and below desorption pressure. *J. Nat. Gas Sci. Eng.* **2017**, *40*, 51–60. [CrossRef]
39. Salmachi, A.; Karacan, C. Özgen Cross-formational flow of water into coalbed methane reservoirs: Controls on relative permeability curve shape and production profile. *Environ. Earth Sci.* **2017**, *76*, 200. [CrossRef]
40. Zhang, C.; Zhang, L. Permeability Characteristics of Broken Coal and Rock under Cyclic Loading and Unloading. *Nonrenew. Resour.* **2019**, *28*, 1055–1069. [CrossRef]
41. Zhang, C.; Zhang, L.; Zhao, Y.; Wang, W. Experimental study of stress–permeability behavior of single persistent fractured coal samples in the fractured zone. *J. Geophys. Eng.* **2018**, *15*, 2159–2170. [CrossRef]